# The Achondroplasia Mutation Does Not Alter the Dimerization Energetics of the Fibroblast Growth Factor Receptor 3 Transmembrane Domain†

Min You, Edwin Li, and Kalina Hristova*

*Department of Materials Science and Engineering, Johns Hopkins University, Baltimore, Maryland 21218*

*Received January 18, 2006; Revised Manuscript Received March 8, 2006*

ABSTRACT: The Gly380 → Arg mutation in the TM domain of fibroblast growth factor receptor 3 (FGFR3) of the RTK family is linked to achondroplasia, the most common form of human dwarfism. The molecular mechanism of pathology induction is under debate, and two different mechanisms have been proposed to contribute to pathogenesis: (1) Arg380-mediated FGFR3 dimer stabilization and (2) slow downregulation of the activated mutant receptors. Here we show that the Gly380 → Arg mutation does not alter the dimerization energetics of the FGFR3 transmembrane domain in detergent micelles or in lipid bilayers. This result indicates that pathogenesis in achondroplasia cannot be explained simply by a higher dimerization propensity of the mutant FGFR3 TM domain, thus highlighting the importance of the observed slow downregulation in phenotype induction.

Achondroplasia, the most common form of short-limbed dwarfism in humans, is an autosomal dominant disorder that interferes with the maturation of the cartilage growth plate of long bones (*1*−*6*). The phenotype is characterized by short stature, diminished muscle tone, narrowing of the lumbar spinal canal, accentuated bowing of the middle and lower part of the back at birth, and trident-shaped hands with a large space between the ring and middle finger. The clinical features of the disorder are due to a defect in chondrocyte function during endochondral bone formation.

Achondroplasia has been associated with the Gly380 → Arg substitution in the TM[1] domain of fibroblast growth factor receptor 3 (FGFR3) in more than 97% of the studied cases (*7*). More than 90% of all cases are sporadic. Mutant alleles exhibit dominance, and the homozygous condition is lethal (*1*).

FGFR3, the membrane protein carrying the achondroplasia mutation, is a receptor tyrosine kinase (RTK) which consists of three extracellular glycosylated Ig-like domains, a transmembrane (TM) domain, and a split cytoplasmic catalytic domain (*8*, *9*). Lateral dimerization of FGFR3, in the presence of ligands (FGFs) and heparin, brings the two cytoplasmic domains in close proximity, resulting in their autophosphorylation and activation (*10*). In long bones, FGFR3 is expressed in proliferating and hypertrophic chondrocytes. FGFR3 null mice exhibit bone overgrowth (*2*, *6*), indicating that FGFR3 is a negative regulator of bone growth. Therefore, the achondroplasia mutation is believed to be a gain-of-function, activating mutation.

Webster and Donoghue have shown that the Gly380 → Arg mutation in FGFR3 enhances the kinase activity of a chimeric Neu/FGFR3 receptor and of FGFR3 (*11*). The authors have proposed that the mutation stabilizes the dimeric state of the receptors, thus promoting unregulated signaling. On the other hand, Monsonego-Ornan and colleagues (*12*) have proposed that a cause for overactivation is the slow downregulation of the mutant receptor. In their study, they found a difference in the rates of internalization and degradation between wild-type and mutant receptors, such that the mutant accumulates at the surface and signals over a longer period of time than the wild type. A recent study by Cho et al. (*13*) confirmed that the degradation of the mutant receptor is compromised. In particular, Cho et al. (*13*) showed that while the wild-type FGFR3 receptor undergoes lysosomal degradation, the mutant receptor is recycled back from the lysosomes to the plasma membrane, thus amplifying FGFR3-mediated signaling. Therefore, it appears that there may exist at least two different mechanisms that contribute to the pathogenesis in achondroplasia, namely, enhanced receptor dimerization and slow receptor downregulation. The relative importance of these two mechanisms in phenotype induction has not been explored in detail.

In our laboratory, we study the biophysical principles behind FGFR3 TM domain dimerization. Previously, we have shown that the FGFR3 TM domain dimerizes in detergent and in lipid bilayers in the absence of the extracellular domains and ligands (*14*). We have also determined the change in the dimerization free energy of the FGFR3 TM domain due to an Ala391 → Glu pathogenic mutation, known as the cause for Crouzon syndrome with acanthosis nigricans (*15*) and cancer (*16*). We have shown that the measured change in free energy of dimerization, $\Delta\Delta G = -1.3$ kcal/mol, can have a dramatic effect on the monomer−dimer equilibrium in lipid bilayers (*17*). Thus, FGFR3 TM dimer stabilization, by itself, could provide a

† This work was supported by NIH Grant GM068619 to K.H.

* To whom correspondence should be addressed: tel, 410-516-8939; fax, 410-516-5293; e-mail, kh@jhu.edu.

[1] Abbreviations: FRET, Förster resonance energy transfer; TM, transmembrane; RTK, receptor tyrosine kinase; FGFR3, fibroblast growth factor receptor 3; Fl, fluorescein; Rhod, rhodamine; POPC, 1-palmitoyl-2-oleoyl-*sn*-glycero-3-phosphocholine; POPS, 1-palmitoyl-2-oleoyl-*sn*-glycero-3-phosphoserine; POPG, 1-palmitoyl-2-oleoyl-*sn*-glycero-3-phosphoglycerol; HFIP, hexafluoro-2-propanol; SDS−PAGE, sodium dodecyl sulfate−polyacrylamide gel electrophoresis.

10.1021/bi060113g CCC: $33.50 
Published on Web 04/06/2006

plausible explanation for the induction of pathological phenotypes due to the Ala391 → Glu mutation (*17*, *18*).

The effect of the achondroplasia mutation on FGFR3 TM domain dimerization has not been studied. Here we measure the free energy of dimerization of the FGFR3 TM domain carrying the Gly380 → Arg mutation and compare it to previously published data for the wild type (*17*). We show that the achondroplasia mutation, unlike the Ala391 → Glu mutation, does not alter the dimerization propensity of the FGFR3 TM domain. Therefore, the phenotype in achondroplasia cannot be correlated simply with stabilization of the mutant TM dimer. This finding points to the importance of slow downregulation of the mutant receptor, in accordance with previous reports of Monsonego-Ornan and colleagues (*12*, *19*) and Cho et al. (*13*).

## MATERIALS AND METHODS

*TM Domain Predictions*. TM domains were identified on the basis of hydropathy analysis. The analysis was carried out using Membrane Protein Explorer (MPEx), a Java applet available over the WWW (http://blanco.biomol.uci.edu/mpex/). MPEx predictions have been shown to be more than 99% correct, when compared against a database of membrane proteins with experimentally verified topologies (*20*).

*Peptide Synthesis*. The TM domains $^{RR}$TM and $^{RR}$TM(R) (see Figure 1 for sequence) were synthesized as previously described (*21*). For the FRET experiments, the single Cys residue in the TM domain, Cys396, was labeled with either fluorescein-maleimide, BODIPY-fluorescein-maleimide, or tetramethylrhodamine-maleimide (Molecular Probes) (*14*). The unreacted dyes were separated from the peptides over an ion-exchange resin, and the labeled peptides were further purified using HPLC. Correct molecular weights were confirmed using MALDI-TOF mass spectrometry. The labeling yields were determined by comparing dye and peptide concentrations as described (*14*). The labeling yield was measured as 95 ± 5%, such that no correction for incomplete labeling was required. The attachment of fluorescent dyes to Cys396, a naturally occurring Cys in the TM domain of FGFR3, has been shown to not perturb the helicity and the dimerization propensity of the TM domain (*14*).

To remove possible TFA ions, complexed with Arg during peptide cleavage and purification, we dissolved the peptide in HCl and then freeze-dried it. This procedure, when repeated several times, has been shown to be effective in removing TFA counterions (*22*−*24*). We found that the procedure does not lead to differences in peptide behavior.

*Circular Dichroism*. CD spectra were recorded in HFIP/TFE, in 4% SDS, and in liposomes. Liposomes were prepared as previously described (*25*, *26*). Briefly, peptides and lipids were premixed in organic solvent, the solvent was removed, and the protein−lipid mixture was hydrated, followed by several freeze−thaw cycles or extrusion. Such liposomes have been shown to be an adequate system for CD and FRET measurements (*26*). The CD spectra were collected using a Jasco spectropolarimeter. The concentrations of the peptides in the samples were determined from absorbance measurements in a Cary 50 (Varian) spectrophotometer.

*Oriented CD.* Oriented CD measurements were performed as previously reported (*27*−*31*). Peptides and lipids were codissolved in HFIP/chloroform. Dropwise, the solution was deposited on a quartz slide, and the solvent was removed under a stream of nitrogen to form a mutilamellar sample containing the peptides. The quartz slide was placed in a custom-designed chamber, such that the multilayers were perpendicular to the beam. To hydrate, a drop of water was placed in the chamber, and the sample was equilibrated for several hours. The sample was rotated around the beam axis in increments of 45°, such that eight spectra were recorded for each sample. The averages and the corresponding standard errors, reported in Figure 3, were obtained from these eight spectra after lipid background corrections.

*SDS*−*PAGE*. About 4 nmol of the peptides was subjected to SDS−PAGE using 10−20% tricine precast gels, following the manufacturer's protocol. NuPAGE reducing agent was used to reduce the samples. The peptides were visualized with Coomassie blue or silver staining.

*Förster Resonance Energy Transfer (FRET).* FRET experiments in vesicles were carried out using a Fluorolog fluorometer (Jobin Yvon) using two donor/acceptor pairs: Fl/Rhod and BODIPY-Fl/Rhod. The Förster radius, $R_0$, is 56 Å for both pairs (*17*). To measure FRET, the excitation wavelength was fixed at 439 nm, and emission spectra were collected from 450 to 800 nm. FRET was measured in liposomes containing known concentrations of donor- and acceptor-labeled proteins as previously described (*14*, *26*). The energy transfer efficiency, $E$, was calculated from measurements of donor intensity at 519 or 515 nm for Fl/Rhod and BODIPY-Fl/Rhod, respectively, according to the equation:

$$E(\%) = (I_D - I_{DA})/(I_D) \times 100 \quad (1)$$

where $I_D$ and $I_{DA}$ are the donor intensities in the absence and in the presence of the acceptor. The measured FRET efficiencies were corrected for FRET arising due to random colocalization of donors and acceptors as described (*14*, *26*).

*Free Energy Calculations.* The association constant $K$ describing the monomer−dimer equilibrium in liposomes depends only on the protein-to-lipid ratio (*26*) and is given by

$$K = [D]/[M]^2 \quad (2)$$

where [D] is the dimer molar concentration in the lipid vesicles (dimers per lipid) and [M] is the monomer molar concentration in the lipid vesicles (monomers per lipid). $K$ is determined by fitting the theoretical FRET efficiencies (or dimer fractions, eq 2) to the experimental data (as in Figure 6). The free energy of dimerization is calculated according to the equation:

$$\Delta G = -RT \ln K \quad (3)$$

## RESULTS

*Prediction of FGFR3 TM Domains and Choice of Peptides for the Study.* The TM domain of fibroblast growth factor receptor 3 (FGFR3) is easy to identify, since it is the most hydrophobic ~19 amino acid long segment. As described in Materials and Methods, we used MPEx (*20*) to identify the segment embedded in the hydrocarbon core of the membrane. According to the prediction, this segment includes

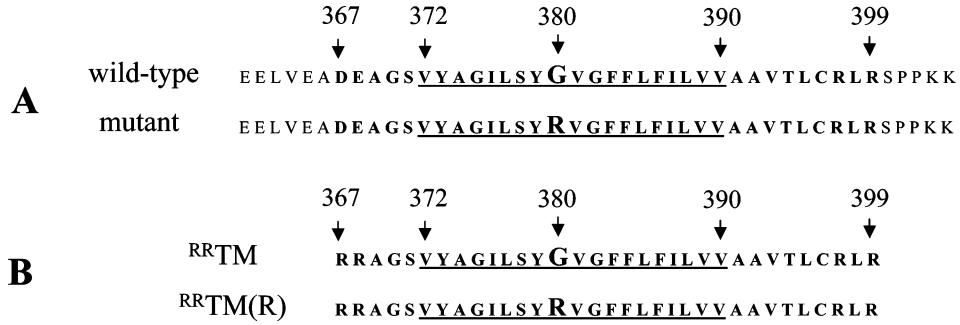


FIGURE 1: (A) Amino acid sequences of wild-type and achondroplasia-causing (mutant) human FGFR3 TM domains. The predicted hydrocarbon core-embedded segments are underlined. (B) Sequences of the two peptides, RRTM and RRTM(R), compared in this study.

residues 372−390 (underlined in Figure 1), and wild-type Gly380 falls in the middle of the bilayer.

To predict the effect of the Gly380 → Arg mutation on FGFR3 topology, we carried out hydropathy analysis of the mutant protein. Although the calculated free energy of TM segment partitioning into the hydrocarbon core increased by ~0.7 kcal/mol due to the mutation, wild-type and mutant proteins were predicted to have identical TM segments (underlined in Figure 1), because the residues surrounding Arg380 are very hydrophobic. This prediction is consistent with recent work (*32*) demonstrating that Arg can indeed partition into the bilayer, if surrounded by hydrophobic residues, as well as with oriented CD spectra presented below.

Like most membrane proteins, the FGFR3 TM domain is flanked by negative charges on the extracellular side and positive charges on the cytoplasmic side (Figure 1A). Therefore, the TM domains could, in principle, form biologically irrelevant antiparallel dimers due to interactions between opposite charges on the C- and N-termini. To eliminate electrostatics as a driving force for dimer formation, we have chosen to work with sequence variants, RRTM and RRTM(R) (see Figure 1B), in which the two negative charges at the N-terminus are substituted with two Arg residues (*17*). This N-terminal substitution does not affect the dimerization of the FGFR3 TM domain in SDS and in liposomes, as shown previously (*17*, *21*) and in Figure 4 below.

*Effect of the Achondroplasia Gly380 → Arg Mutation on Secondary Structure and Membrane Disposition.* To evaluate the structural consequences of the Gly380 → Arg mutation in the FGFR3 TM domain, we first investigated if the mutation affects the helicity of RRTM in organic solvent and in SDS. The solution CD spectra of RRTM and RRTM(R) in TFE/HFIP (2:1) and in 4% SDS are shown in Figure 2A,B. The CD spectra of the two peptides are very similar, suggesting that the mutation does not cause a loss of helicity. The CD spectra of RRTM and RRTM(R) in POPC vesicles, shown in Figure 2C, are also very similar, suggesting that the secondary structures of RRTM and RRTM(R) in lipid bilayers are similar.

Next, we investigated if the Gly380 → Arg mutation perturbs the TM orientation of the peptide using oriented CD (OCD). Figure 3 shows the expected theoretical OCD spectra for helices that are normal (solid black curve) and parallel (dashed black curve) to the membrane plane (*33*). The experimental OCD spectra for RRTM and RRTM(R) (blue and red curves, respectively, in Figure 3) in oriented POPC multilayers are the averages for eight different rotation angles

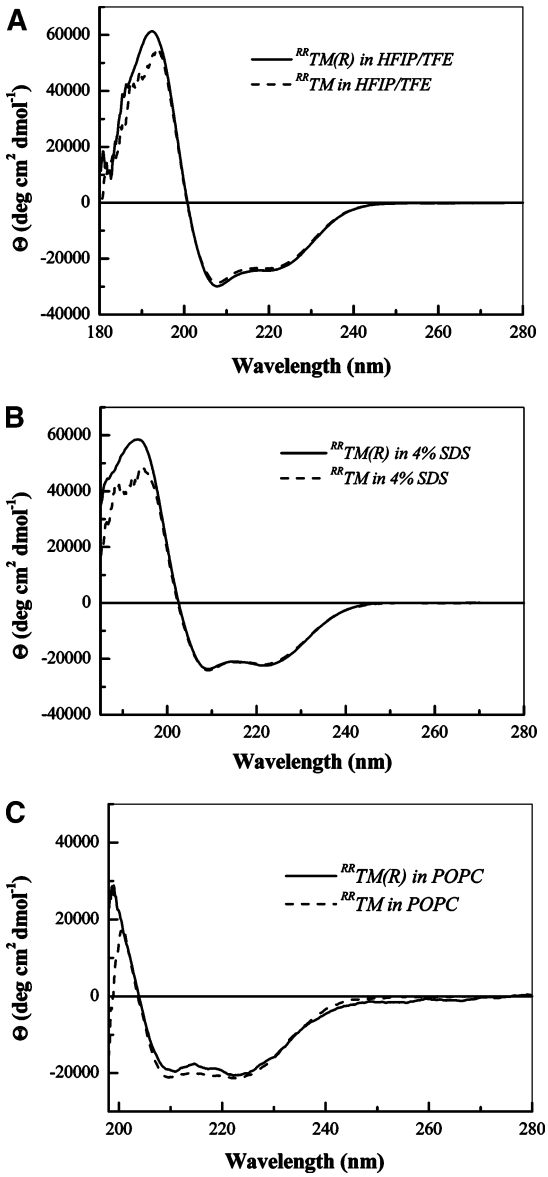


FIGURE 2: (A) CD spectra of RRTM(R) and RRTM in HFIP/TFE. (B) CD spectra of RRTM(R) and RRTM (*17*) in 4% SDS. (C) CD spectra of RRTM(R) and RRTM (*17*) in POPC vesicles. RRTM(R) is helical in all hydrophobic environments, and the achondroplasia mutation has no significant effect on helicity.

(see Materials and Methods). The comparison between theory and experiment demonstrates that both RRTM and RRTM(R) adopt transmembrane orientation. Therefore, the mutation does not induce a measurable (by OCD) change in bilayer disposition.

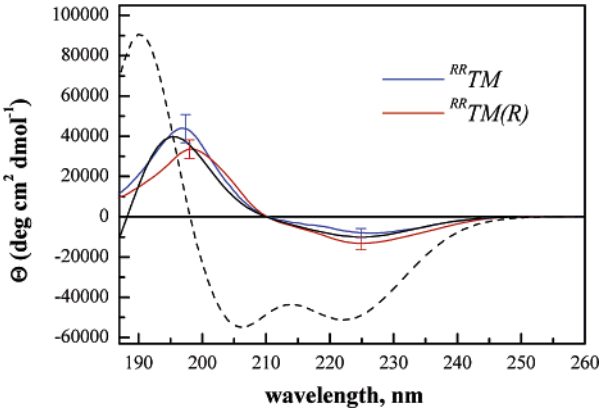


FIGURE 3: Oriented CD spectra of $^{RR}$TM(R) (red) and $^{RR}$TM (blue; data from ref *17*) in POPC multilayers. Peptides and lipids (molar ratio 1:20) were mixed in HFIP/chloroform, deposited on a quartz slide, and hydrated to form multilayers. The experimental spectra, obtained from eight discrete scans, are compared to theoretical spectra of helices that are normal (black solid line) and parallel (black dashed line) to the membrane plane. Both $^{RR}$TM(R) and $^{RR}$TM are transmembrane, and the achondroplasia mutation has no significant effect on helix tilt.

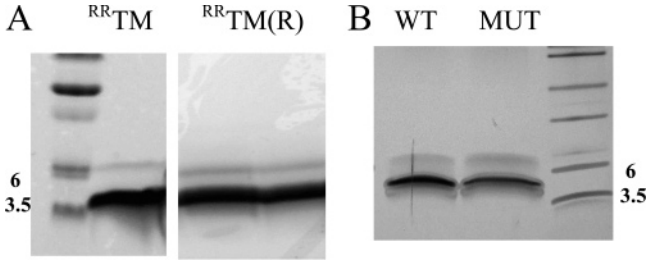


FIGURE 4: FGFR3 TM domain dimerization in SDS. Peptides, dissolved in sample buffer, were reduced with NuPAGE reducing agent and boiled for 5 min prior to loading onto Novex precast tricine gels. (A) Results for $^{RR}$TM(R) and $^{RR}$TM. (B) Results for the naturally occurring TM domain sequences for the wild type and mutant, containing two negatively charged amino acids (ED) at the N-terminus (see Figure 1A for sequences). The intensities of the dimeric bands are not affected by the achondroplasia mutation.

*Effect of the Achondroplasia Gly380 → Arg Mutation on Dimerization, Studied by SDS−PAGE.* SDS−PAGE has been shown to adequately report dimerization propensities of TM domain variants (*34*−*36*) and of FGFR3 variants in particular. While SDS−PAGE cannot be used to gain precise thermodynamic information about the dimerization process, an apparent free energy of dimerization could be determined by measuring the monomer and dimer fractions. We have previously demonstrated that the Ala391 → Glu mutation stabilizes the FGFR3 TM dimer in SDS by ∼−1.7 kcal/mol (*17*).

To study the effect of the achondroplasia mutation on dimerization, we subjected $^{RR}$TM(R) to SDS−PAGE, together with $^{RR}$TM for comparison. Typical SDS−PAGE results for $^{RR}$TM and $^{RR}$TM(R) are shown in Figure 4A. Two distinct bands, corresponding to monomers and dimers, were observed for both $^{RR}$TM and $^{RR}$TM(R). The intensities of the dimeric bands of $^{RR}$TM and $^{RR}$TM(R) are very similar, suggesting that the mutation does not affect the stability of the dimer. This result is not affected by the N-terminal sequence modification of the peptides: the SDS gels of $^{RR}$TM and $^{RR}$TM(R) in Figure 4A are very similar to gels of the naturally occurring TM domain sequences for the wild type and mutant (Figure 4B), containing two negatively charged amino acids (ED) at the N-terminus (see Figure 1 for sequence details).

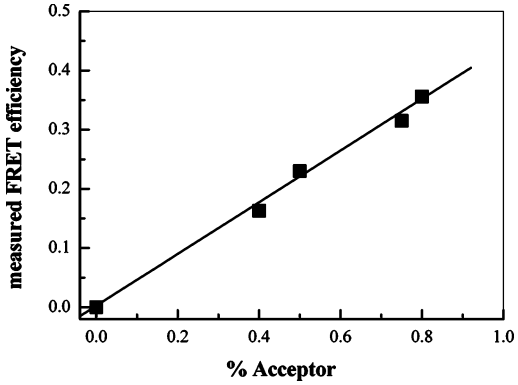


FIGURE 5: Measured FRET efficiency for $^{RR}$TM(R) as a function of acceptor mole ratio. The peptide-to-lipid ratio was kept constant at 1:500, while the ratio of donor-labeled to acceptor-labeled peptides was varied. The linear dependence of the energy transfer on the acceptor mole ratio is indicative of dimer formation.

*Effect of the Mutation on Dimerization in Liposomes, Studied with Förster Resonance Energy Transfer (FRET).* FRET is another powerful tool for probing dimerization, and it can be measured in liposomes, an environment that mimics the biological membrane (*26*). Using FRET, we have previously demonstrated a weak dimerization propensity for the wild-type FGFR3 TM domain (*14*). We have also shown that the pathogenic Ala391 → Glu mutation, a mutation known as the cause for Crouzon syndrome with acanthosis nigricans (*15*) and cancer (*16*), stabilizes the FGFR3 TM dimer by −1.3 kcal/mol and induces a large shift in the equilibrium between monomers and dimers (*17*).

To determine the dimerization propensity of $^{RR}$TM(R), we carried out FRET measurements using two different sets of FRET pairs, fluorescein/rhodamine (Fl/Rhod) and BODIPY-fluorescein/rhodamine (BODIPY-Fl/Rhod), and compared the results to previous measurements of the wild type (*17*). We recorded spectra of donor- and acceptor-labeled $^{RR}$TM(R) in liposomes, as well as control samples of donor-labeled $^{RR}$TM(R), as described (*14*). The FRET efficiency was calculated from the decrease in donor fluorescence using eq 1.

First, FRET was measured for a constant peptide-to-lipid ratio but varying donor-to-acceptor ratio. The linear dependence of the energy transfer on the acceptor mole ratio, shown in Figure 5, is indicative of dimer formation. Therefore, $^{RR}$TM(R) exists in a monomer−dimer equilibrium and does not form higher order aggregates (*25*, *26*, *37*, *38*), similar to the wild type (*14*).

To calculate the dimer fraction and the free energy of dimerization of $^{RR}$TM(R), we followed a previously described protocol (*26*). The FRET that arises due to random proximity effects was modeled according to the analysis of Wolber and Hudson (*39*). Then, the predicted FRET efficiency due to proximity was subtracted from the measured FRET signal to obtain the FRET efficiency due to sequence-specific dimerization (*26*). The results are shown in Figure 6 for a donor-to-acceptor ratio of 1. The solid squares represent the measured FRET efficiency due to sequence-specific dimerization, or the dimer fraction [D]/(2[D] + [M]), for $^{RR}$TM(R) as a function of total peptide concentration, (2[D] + [M]).

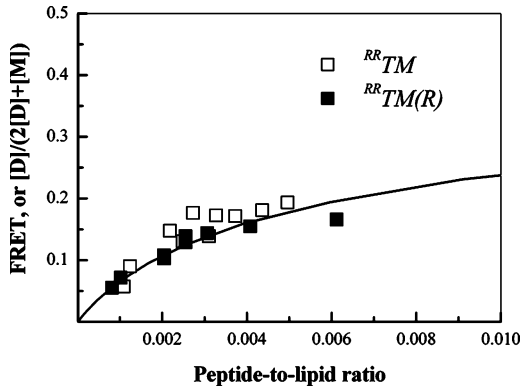


FIGURE 6: Energetics of $^{RR}$TM(R) dimerization in POPC. In this experiment, the peptide-to-lipid ratio was varied, while the ratio of donor-labeled to acceptor-labeled peptides was kept constant at 1:1. The FRET efficiencies due to sequence-specific dimerization of $^{RR}$TM(R) (solid squares) were calculated as described in Materials and Methods. The free energy of $^{RR}$TM(R) dimerization, $\Delta G = -2.7$ kcal/mol, was determined by fitting the theoretical curve (solid line) to the experimental data (solid squares) (*14*, *26*). The data for wild-type $^{RR}$TM (*17*) are shown for comparison. The dimer fractions measured for $^{RR}$TM and $^{RR}$TM(R) are very similar, and therefore the achondroplasia mutation does not alter the stability of the FGFR3 TM dimer in POPC bilayers.

Table 1: Dimer Fraction of $^{RR}$TM(R), for 0.2 mol % Total Peptide Concentration, as a Function of Lipid Composition

| lipid composition | dimer fraction, [D]/(2[D] + [M]) |
|---|---|
| 100% POPC | 0.11 ± 0.03 |
| 80% POPC + 20% POPS | 0.10 ± 0.04 |
| 75% POPC + 25% POPG | 0.09 |
| 75% POPC + 25% POPS | 0.09 ± 0.04 |
| 90% POPC + 10% cholesterol | 0.09 ± 0.03 |

For comparison, we also show the data for wild-type $^{RR}$TM (open squares).

The $^{RR}$TM(R) association constant $K$ was determined by fitting the theoretical equilibrium curve derived from eq 2 (solid line) to the experimental data (solid squares). Two different fitting procedures were used, as previously described (*17*). First, $R_0$ was fixed at 56 Å [a value that we have previously measured for the two donor/acceptor pairs used, fluorescein/rhodamine and BODIPY-fluorescein/rhodamine (*17*)], such that the only varied parameter was $K$, or the free energy of dimerization $\Delta G = -RT \ln K$. This gave $\Delta G = -2.7$ kcal/mol. Then, we subjected the data to a two-parameter fit by simultaneously varying $K$ (or $\Delta G$) and $R_0$ (or the predicted FRET due to random colocalization of donors and acceptors). This procedure gave $\Delta G = -2.8$ kcal/mol and $R_0 = 52$ Å. This result did not depend on the initial guesses for $\Delta G$ and $R_0$, indicative of a unique robust fit. On the basis of these results, the free energy of dimerization of $^{RR}$TM(R) is $\Delta G = -2.7 \pm 0.1$ kcal/mol, identical (within experimental error) to the free energy of dimerization measured for $^{RR}$TM, $-2.8 \pm 0.1$ kcal/mol (*17*). Therefore, we find that the achondroplasia mutation does not alter the stability of the FGFR3 TM dimer in liposomes.

*Effect of Lipid Composition on $^{RR}$TM(R) Dimerization.* Finally, we measured the FRET efficiencies for $^{RR}$TM(R) in liposomes containing different lipids (POPC, POPS, POPG, and cholesterol). The measured FRET efficiencies and the calculated dimer fractions (Table 1) do not depend on the lipid compositions. Similar results have been obtained for $^{RR}$TM and the Ala391 → Glu mutant (*17*). Thus, it appears that the dimerization propensities of the FGFR3 TM domain and its pathogenic mutants are not very sensitive to lipid composition.

## DISCUSSION

*FGFR3 TM Dimer Stability in Achondroplasia.* We have shown that the dimerization propensity of the FGFR3 TM domain does not change in the presence of the achondroplasia Gly380 → Arg mutation. This result, derived from SDS−PAGE and FRET measurements in liposomes, differs from previous findings about a pathogenic Ala391 → Glu mutation in the same protein (*17*). While the Ala391 → Glu mutation stabilizes the FGFR3 TM dimer by −1.3 kcal/mol, the achondroplasia Gly380 → Arg mutation has no effect on dimer stability. Therefore, pathogenesis in achondroplasia cannot be simply a consequence of enhanced mutant TM dimer stability.

*Mechanism of Pathology Induction in Achondroplasia.* Webster and Donoghue have demonstrated that the Gly380 → Arg mutation in FGFR3 dramatically increases the autophosphorylation of a chimeric Neu/FGFR3 receptor and induces cell transformation (*11*). The mutation also causes constitutive activation of FGFR3 (*11*), without interfering with the correct localization of the receptor on the plasma membrane. On the basis of these results, the authors have proposed that the molecular basis of achondroplasia is unregulated signal transduction due to enhanced receptor dimerization. Here we measure the dimerization propensity of the FGFR3 TM domain carrying the achondroplasia mutation. Surprisingly, we find that the dimerization propensities of the wild-type and mutant FGFR3 TM domains are the same, and therefore it appears that the observations of Webster and Donoghue cannot be explained simply by Arg380-mediated TM dimer stabilization.

Monsonego-Ornan and colleagues (*12*) have reported that the mutant receptor is downregulated very slowly. The authors found that FGFR3 is not efficiently degraded, despite being ubiquitinated at a higher level (*19*) and exhibiting higher tyrosine phosphorylation. As a result, the mutant receptor accumulates at the surface and signals over a longer period of time than the wild type, thus amplifying the signal. A later study showed that FGFR3 receptors, carrying the achondroplasia mutation, escape lysosomal degradation and are recycled back to the plasma membrane, thus prolonging the lifetime of the activated receptors (*13*). It therefore appears that a defect in downregulation is an important contributor to pathogenesis in achondroplasia. Our finding that the achondroplasia mutation does not stabilize the TM domain dimer further highlights the importance of slow downregulation in pathogenesis. Future studies should focus on the molecular basis of the compromised downregulation of the mutant receptor.

## ACKNOWLEDGMENT

We thank Xue Han for technical assistance. We also thank Drs. Jay Gargus, Daniel Donoghue, and Clair Francomano for stimulating discussions.

## REFERENCES

1. Vajo, Z., Francomano, C. A., and Wilkin, D. J. (2000) The molecular and genetic basis of fibroblast growth factor receptor

3 disorders: The achondroplasia family of skeletal dysplasias, Muenke craniosynostosis, and Crouzon syndrome with acanthosis nigricans, *Endocr. Rev. 21*, 23−39.
2. Deng, C., Wynshaw-Boris, A., Zhou, F., Kuo, A., and Leder, P. (1996) Fibroblast growth factor receptor 3 is a negative regulator of bone growth, *Cell 84*, 911−921.
3. Nguyen, H. B., Estacion, M., and Gargus, J. J. (1997) Mutations causing achondroplasia and thanatophoric dysplasia alter bFGF-induced calcium signals in human diploid fibroblasts, *Hum. Mol. Genet. 6*, 681−688.
4. Ponseti, I. V. (1970) Skeletal growth in achondroplasia, *J. Bone Jt. Surg., Am. Vol. A 52*, 701.
5. Maynard, J. A., Ippolito, E. G., Ponseti, I. V., and Mickelson, M. R. (1981) Histochemistry and ultrastructure of the growth plate in achondroplasia, *J. Bone Jt. Surg., Am. Vol. 63*, 969−979.
6. Colvin, J. S., Bohne, B. A., Harding, G. W., Mcewen, D. G., and Ornitz, D. M. (1996) Skeletal overgrowth and deafness in mice lacking fibroblast growth factor receptor 3, *Nat. Genet. 12*, 390−397.
7. Shiang, R., Thompson, L. M., Zhu, Y.-Z., Church, D. M., Fielder, T. J., Bocian, M., Winokur, S. T., and Wasmuth, J. J. (1994) Mutations in the transmembrane domain of FGFR3 cause the most common genetic form of dwarfism, achondroplasia, *Cell 78*, 335−342.
8. Wilkie, A. O. M., Morriss-Kay, G. M., Jones, E. Y., and Heath, J. K. (1995) Functions of fibroblast growth factors and their receptors, *Curr. Biol. 5*, 500−507.
9. L'Horte, C. G. M., and Knowles, M. A. (2005) Cell responses to FGFR3 signaling: growth, differentiation and apoptosis, *Exp. Cell Res. 304*, 417−431.
10. Spivakkroizman, T., Lemmon, M. A., Dikic, I., Ladbury, J. E., Pinchasi, D., Huang, J., Jaye, M., Crumley, G., Schlessinger, J., and Lax, I. (1994) Heparin-induced oligomerization of Fgf molecules is responsible for Fgf receptor dimerization, activation, and cell-proliferation, *Cell 79*, 1015−1024.
11. Webster, M. K., and Donoghue, D. J. (1996) Constitutive activation of fibroblast growth factor receptor 3 by the transmembrane domain point mutation found in achondroplasia, *EMBO J. 15*, 520−527.
12. Monsonego-Ornan, E., Adar, R., Feferman, T., Segev, O., and Yayon, A. (2000) The transmembrane mutation G380R in fibroblast growth factor receptor 3 uncouples ligand-mediated receptor activation from down-regulation, *Mol. Cell. Biol. 20*, 516−522.
13. Cho, J. Y., Guo, C. S., Torello, M., Lunstrum, G. P., Iwata, T., Deng, C. X., and Horton, W. A. (2004) Defective lysosomal targeting of activated fibroblast growth factor receptor 3 in achondroplasia, *Proc. Natl. Acad. Sci. U.S.A. 101*, 609−614.
14. Li, E., You, M., and Hristova, K. (2005) SDS−PAGE and FRET suggest weak interactions between FGFR3 TM domains in the absence of extracellular domains and ligands, *Biochemistry 44*, 352−360.
15. Meyers, G. A., Orlow, S. J., Munro, I. R., Przylepa, K. A., and Jabs, E. W. (1995) Fibroblast-growth-factor-receptor-3 (Fgfr3) transmembrane mutation in Crouzon-syndrome with acanthosis nigricans, *Nat. Genet. 11*, 462−464.
16. van Rhijin, B., van Tilborg, A., Lurkin, I., Bonaventure, J., de Vries, A., Thiery, J. P., van der Kwast, T. H., Zwarthoff, E., and Radvanyi, F. (2002) Novel fibroblast growth factor receptor 3 (FGFR3) mutations in bladder cancer previously identified in non-lethal skeletal disorders, *Eur. J. Hum. Genet. 10*, 819−824.
17. Li, E., You, M., and Hristova, K. (2006) FGFR3 dimer stabilization due to a single amino acid pathogenic mutation, *J. Mol. Biol. 356*, 600−612.
18. Merzlyakov, M., You, M., Li, E., and Hristova, K. (2006) Transmembrane helix heterodimerization in lipids bilayers: probing the energetics behind autosomal dominant growth disorders, *J. Mol. Biol. 358*, 1−7.
19. Monsonego-Ornan, E., Adar, R., Rom, E., and Yayon, A. (2002) FGF receptors ubiquitylation: dependence on tyrosine kinase activity and role in downregulation, *FEBS Lett. 528*, 83−89.
20. Jayasinghe, S., Hristova, K., and White, S. H. (2001) Energetics, stability, and prediction of transmembrane helices, *J. Mol. Biol. 312*, 927−934.
21. Iwamoto, T., You, M., Li, E., Spangler, J., Tomich, J. M., and Hristova, K. (2005) Synthesis and initial characterization of FGFR3 transmembrane domain: Consequences of sequence modifications, *Biochim. Biophys. Acta 1668*, 240−247.
22. Sharon, M., Oren, Z., Shai, Y., and Anglister, J. (1999) 2D-NMR and ATR-FTIR study of the structure of a cell-selective diastereomer of melittin and its orientation in phospholipids, *Biochemistry 38*, 15305−15316.
23. Hetru, C., Letellier, L., Oren, Z., Hoffmann, J. A., and Shai, Y. (2000) Androctonin, a hydrophilic disulphide-bridged non-haemolytic anti-microbial peptide: a plausible mode of action, *Biochem. J. 345*, 653−664.
24. Brazier, S. P., Ramesh, B., Haris, P. I., Lee, D. C., and Srai, S. K. S. (1998) Secondary structure analysis of the putative membrane-associated domains of the inward rectifier $K^+$ channel ROMK1, *Biochem. J. 335*, 375−380.
25. Li, E., and Hristova, K. (2004) Imaging FRET measurements of transmembrane helix interactions in lipid bilayers on a solid support, *Langmuir 20*, 9053−9060.
26. You, M., Li, E., Wimley, W. C., and Hristova, K. (2005) FRET in liposomes: measurements of TM helix dimerization in the native bilayer environment, *Anal. Biochem. 340*, 154−164.
27. Vogel, H. (1987) Comparison of the conformation and orientation of alamethicin and melittin in lipid membranes, *Biochemistry 26*, 4562−4572.
28. Olah, G. A., and Huang, H. W. (1988) Circular dichroism of oriented α helices. I. Proof of the exciton theory, *J. Chem. Phys. 89*, 2531−2538.
29. Olah, G. A., and Huang, H. W. (1988) Circular dichroism of oriented α helices. II. Electric field oriented polypeptides, *J. Chem. Phys. 89*, 6956−6962.
30. Hristova, K., Wimley, W. C., Mishra, V. K., Anantharamaiah, G. M., Segrest, J. P., and White, S. H. (1999) An amphipathic α-helix at a membrane interface: A structural study using a novel X-ray diffraction method, *J. Mol. Biol. 290*, 99−117.
31. Hristova, K., Dempsey, C. E., and White, S. H. (2001) Structure, location, and lipid perturbations of melittin at the membrane interface, *Biophys. J. 80*, 801−811.
32. Hessa, T., White, S. H., and von Heijne, G. (2005) Membrane insertion of a potassium-channel voltage sensor, *Science 307*, 1427.
33. Wu, Y., Huang, H. W., and Olah, G. A. (1990) Method of oriented circular dichroism, *Biophys. J. 57*, 797−806.
34. Lemmon, M. A., Flanagan, J. M., Hunt, J. F., Adair, B. D., Bormann, B. J., Dempsey, C. E., and Engelman, D. M. (1992) Glycophorin-A dimerization is driven by specific interactions between transmembrane α-helices, *J. Biol. Chem. 267*, 7683−7689.
35. Russ, W. P., and Engelman, D. M. (1999) TOXCAT: A measure of transmembrane helix association in a biological membrane, *Proc. Natl. Acad. Sci. U.S.A. 96*, 863−868.
36. Sulistijo, E. S., Jaszewski, T. M., and MacKenzie, K. R. (2003) Sequence-specific dimerization of the transmembrane domain of the "BH3-only" protein BNIP3 in membranes and detergent, *J. Biol. Chem. 278*, 51950−51956.
37. Adair, B. D., and Engelman, D. M. (1994) Glycophorin a helical transmembrane domains dimerize in phospholipid bilayers—a resonance energy transfer study, *Biochemistry 33*, 5539−5544.
38. Li, M., Reddy, L. G., Bennett, R., Silva, N. D., Jr., Jones, L. R., and Thomas, D. D. (1999) A fluorescence energy transfer method for analyzing protein oligomeric structure: Application to phospholamban, *Biophys. J. 76*, 2587−2599.
39. Wolber, P. K., and Hudson, B. S. (1979) An analytic solution to the Förster energy transfer problem in two dimensions, *Biophys. J. 28*, 197−210.

BI060113G